Design of Tidal Range Energy Generation Schemes using a Genetic Algorithm Model

Jingjing Xue[1], Dr. Reza Ahmadian[2], Prof. Owen Jones[3], Prof. Roger A. Falconer[4]
[1, 2 and 4] *Cardiff School of Engineering, Queen's Building, The Parade, Cardiff, U.K. CF24 3AA*
[3] *Cardiff School of Mathematics Cathays, Cardiff, U.K. CF24 4AG*
[1]*XueJ7@cf.ac.uk*
[2]*AhmadianR@cf.ac.uk*
[3]*joneso18@cf.ac.uk*
[4]*FalconerRA@cf.ac.uk*

Abstract

One of the key aspects of Tidal Range Schemes globally is identifying the most appropriate site and the optimised design and operation of the scheme, to maximise societal needs and the benefits from electricity generation. Variations in the design parameters of Tidal Range Schemes for electricity generation could therefore lead to a very large number of design and operation scenarios. In this study, a novel Genetic Algorithm model was developed to deliver the complete design of the most optimised Tidal Range Schemes for electricity generation, including the number of turbines, sluicing areas and the maximum amount of electricity that could be generated, through identifying the most optimised operation scheme for a particular site. The Genetic Algorithm model has been used to design a new Tidal Range Scheme proposed for development in the Bristol Channel, UK, with a potential to generate about 7.16 TWh/yr. The design of the scheme was also investigated using a traditional grid search approach for a range of scenarios, together with the model being used to investigate the performance of the complete design of the scheme, evaluated through a comparison of the most optimised design in terms of electricity generation. This comparison has shown that the Genetic Algorithm model was capable of achieving largely the same outcomes and reducing the computational time by approximately 95% to that based on using traditional Grid Search methods.

Keywords: Tidal Energy; Tidal Lagoons; Tidal Barrages; Genetic Algorithms; Operational Optimisation; Tidal Dynamics

1. Introduction

Reducing Green House Gas (GHGs) emissions in order to slow down and potentially control the impact of climate change has been one the biggest public concerns and one of the greatest challenges for governments and researchers world-wide in recent years [1, 2]. Various types of renewable energy options have been implemented world-wide, such as wind, solar and hydropower, to contribute to the global energy mix [3]. Moreover, there are other less exploited sources of renewable energy which are now also being developed [3, 4]. One of these less developed sources is tidal energy, which is estimated to have the potential to provide a significant amount of energy in various parts of the world [5]. For example, one of the main types of methods of producing tidal energy consists of tidal range schemes (TRSs), with the potential to provide up to 20% of the UK's current electricity demand [6]. These schemes (including barrages and lagoons) are designed to create an artificial head difference across an impoundment wall along an estuary or coastline, with energy being generated from this head difference by converting the potential energy to kinetic energy, and then delivering mechanical and electrical energy through turbines.

In the early stages of the design process, the predicted energy generated by such a proposed scheme, and its optimisation, is carried out using simplified 0-D models. This is due to the significantly reduced computational cost of using such models in comparison with conventional 2-D and 3-D hydro-environmental models. These 0-D models

considerably simplify the complex tidal hydrodynamic processes by considering mass conservation only [7, 8]. The details of 0-D modelling are provided in section 4.4. 0-D modelling was first used for designing the operation of TRSs by Prandle [9]. He used a fixed operation scheme, which meant that the scheme always operated under the same starting and ending head differences, regardless of the variability of the tidal characteristics [10], such as amplitude, throughout the spring-neap cycle [11] and the year [12, 13]. More recently, it has been shown that a flexible operation of TRSs could increase the annual energy output from such schemes, including barrages and lagoons, which means that the operational head could be varied during spring and neap tides and during flood and ebb tides [14-16]. Widely available 0-D models use different optimisation approaches, including the gradient-based method [7, 17] and the grid search method [16], with both methods being developed to optimise the operation of TRSs. It has been shown that the flexible operation of TRSs, which use different starting and ending heads at each operation phase, could increase the annual electricity generated by typically 10% [16]. However, one of the key challenges in the operational design of TRSs is the various design variables of the scheme, including: basin size, number of turbines and sluice gate area and the operation schedule. Therefore, the optimal design of a scheme requires a large number of simulations to be undertaken, due to the multi-parameter nature of such schemes for optimisation. This simplified approach provides a higher level of uncertainty in the early stages of design, which can be refined further as the design progresses using either 2-D or 3-D hydrodynamic modelling tools. Optimisation of the entire scheme with some degree of confidence is particularly crucial in the early stages of operational design, due to the significant influence of these multi-variables on maximising the annual electricity generated and therefore the feasibility of any proposed scheme [18]. Hence, a more advanced optimisation algorithm with high computational efficiency, and which provides more certainty of the operational outputs of a scheme through a cost-benefit analysis, is needed to facilitate the development and operational design of TRSs, particularly in terms of maximising energy generation to meet demand.

Evolutionary Algorithms (EAs) have been developed to solve a wide range of optimisation problems in power systems [19, 20], with Genetic Algorithms (GAs) constituting one of the metaheuristic EAs frequently used to combine variables to analyse optimisation problems, and providing a high level of satisfactory results [21], especially when compared with the brute force algorithms including the grid search method [22]. EAs have been used in the optimisation of tidal energy generated from TRSs, and have already been used to provide design details in terms of the number of turbines and sluice gates to use for such schemes [18, 23, 24]. Leite Neto et al. discussed the maximum energy gains obtained with dispatchable turbines by using GAs for optimisation [24]. They investigated the potential of using GAs to optimise the operation of such schemes [24]. More recently, GAs have been refined to determine operational optimisation with the findings being possible for the implementation of GAs in the optimal design of TRSs for higher efficiency [17], particularly in comparison with other alternative algorithms [18]. Furthermore, Kontoleontos and Weissenberger [23] highlighted the scope for using EAs in optimising multiple variables, including operational modes, speed of turbines etc., to maximise energy generation. However, so far as the authors are aware no studies have been published to-date using GAs, or similar EAs, in simultaneously designing and optimising TRSs, where different numbers and combinations of turbines and sluice gates have been considered, as well as consideration being given to flexible operation linked to the tidal characteristics and pumping at high and low water to increase energy generation. The focus of this study is therefore to investigate and address these additional considerations to optimise tidal energy to meet demand.

The aims of this paper are therefore to: (a) develop a GA model to carry out the complete design of a TRS and its application to a large Tidal Lagoon proposed to be built in the UK, namely the West Somerset Lagoon (WSL), (b) illustrate the GA model performance for multi-variable optimisation and compare the results with a more elaborate and time-consuming grid search approach, and (c) validate the applicability of the optimum schemes driven by the GA model, using a 0-D model, and by simulating the optimum schemes using a more sophisticated 2-D unstructured grid model, namely the Depth Integrated Velocities And Solute Transport (DIVAST 2-DU) model.

2. Tidal Range Schemes

A Tidal Range Scheme can be designed under various operation modes, including generating electricity during flood-only, ebb-only or 2-way generation. One of the most efficient tidal range operation schemes, which has been adopted in many TRSs [11, 25, 26], is 2-way generation, where electricity is generated during both flood and ebb tides and provides a longer period of generation through the tidal cycle.

A full operating process includes three main stages, as follows: (i) holding phase: this mode starts when the water level inside the impoundment is almost the same as the water level on the seaward side of the structure. Both the turbines and sluices are kept closed during this phase, thereby keeping the basin water level unchanged until a sufficient head difference for efficient electricity generation is achieved across the structure; (ii) generation phase: this mode commences when the head difference across the structure reaches a pre-set value, i.e., H_{se} for ebb tides or H_{sf} for flood tides, as shown in Figure 1. During this phase, the turbines are operating and generating electricity, while the sluice gates are kept closed; (iii) sluicing phase: when the head difference across the structure drops below a specific predetermined value or ending head, i.e., H_{ee} for ebb tides or H_{ef} for flood tides, then the sluicing phase starts. During this phase, both the turbines and sluices are open, thereby allowing more water to flow into, or out of, the impoundment to generate a larger head difference during the next generating phase. The next holding phase starts by closing the sluice gates and turbines, when the water levels on both sides of the structure are almost the same.

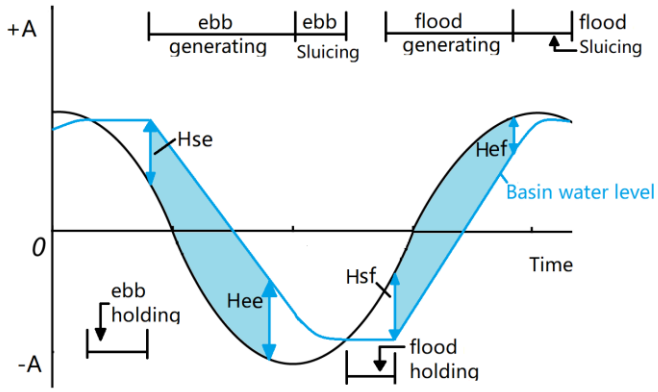

Fig. 1. Schematic representation of the operation (excluding pumping) for two-way tidal energy generation.

Pumping can be added as part of the operation to increase the energy generated by increasing the operating head [27]. Pumping starts, by reverse operation of the turbines, following the sluicing phase and increases or decreases the water levels in the impoundment to a predefined pumping height, namely H_{pe} for ebb tides or H_{pf} for flood tides.

3. West Somerset Lagoon

The Bristol Channel and Severn Estuary are located in the South West of the UK and separate Wales from England. In addition to having very large tidal ranges, i.e., the second largest tidal range world-wide, the basin is also close to urban areas of high energy demand. Therefore this coastal basin has been considered for the development of a number of TRSs, particularly with the Severn Barrage being considered in some detail since the 1930s [28, 29]. A more recent scheme has been proposed in the form of a 14 km diameter lagoon, namely the West Somerset Lagoon (WSL), which is located in the Bristol Channel close to Minehead, with the scheme being promoted by Tidal Engineering and Environmental Services Ltd. (TEES) [30]. WSL includes an impoundment wall, approximately 22 km in length, from Culver Cliff in Minehead to Blue Ben Point at West Quantox Head. The basin impounds approximately 80 km^2 of coastal waters [30], as shown in Figure 2. The life of the project is expected to be at least 120 years and, according to the developers, the scheme will also act as a sea defence and combat coastal erosion and future flooding, in addition to generating tidal renewable energy [30]. The scheme could also complement other proposed schemes around the UK, with the different times of high tide around the UK coast providing complementary and predictable tidal energy contributions to the grid. There are significant differences in tidal phases and ranges at the sites suitable for TRSs

around the UK. TRS operators can exploit these difference and predictability of the tides and operate multiple TRSs in harmony to provide the electricity network with different ancillary services, baseload or storage [31, 59].

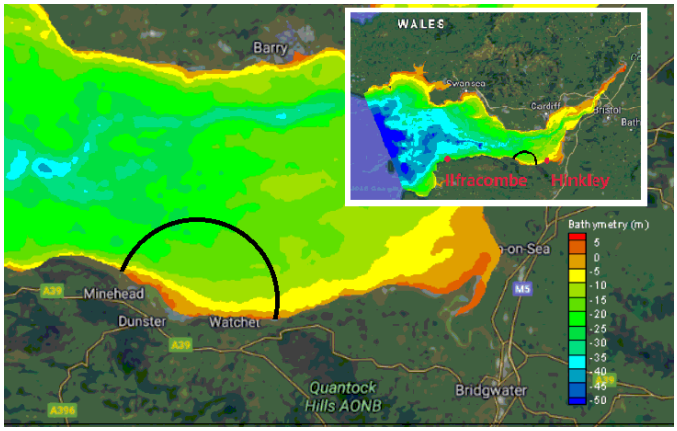

Fig.2. Map of the Bristol Channel, the black line shows the location of the West Somerset Lagoon along the south west coast of England from Google Map [30]. The validation points of Hinkley and Ilfracombe in the 2-D model were marked as red dots.

4. The GA model

4.1. Genetic Algorithm

Genetic Algorithms (GAs) are evolutionary search algorithms that are used to solve optimisation challenges by iterations. The nature of GAs is to simulate the process of natural selection [32] by continuously evolving and improving the population [33]. In GAs, each individual represents a solution with a string of the encoded parameters of the computational model, which are called genes or chromosomes [34], while a population of individuals shapes a generation. GA models begin with a randomly generated population of individuals (known as 'children' in the current generation). These individuals then go through three sequential events or processes to generate the next generation. The key processes applied are mutation, recombination and selection, which are considered with the probabilities of P_m, P_r and P_s [20, 35], respectively.

In the process of mutation, the new attributes can be created at any place in the genes. In the recombination process, any two parts of randomly selected genes can be crossed over and generate two new genes. There are a variety of mutation and recombination methods used in GA approaches. It has been shown that implementing a Sequence Mutation Method (SMM) and a Ring Recombination Method (RRM) [18, 36] can lead to better optimisation results with higher efficiency, in comparison to other methods [20, 37]. The mutation will restart from the first gene in the next generation when the end of the gene sequence of an individual is reached during the mutation. This process is repeated as the evolution continues. The 'Ring' in RMM denotes that chromosomes of individuals are considered in a ring form [18, 38, 39] and a random section of the chromosomes are selected, which is not limited to the length of the chromosome. All individuals are evaluated using a fitness function before the next generation is produced. Individuals with higher fitness values have more chance of surviving and being promoted to the next generation as a community of 'Parents'. This process is iterated until the stopping criterion is reached [40], as introduced in section 4.4.

4.2. Introduction to the GA model

The GA model was set-up mimicking the process of GAs to optimise the operation of a TRS. For the process of mutation, the new scheme would be created from the schemes which survived from the previous generation by randomly mutating the values of various parameters in the schemes and then, in the process of recombination, the

selected schemes would be genetically recombined. This was followed by the energy generated from all schemes being calculated over the selected typical tidal cycle. Based on the principle of ‘survival of the fittest’, the schemes with a greater level of energy generation survived, while the ‘weaker’ schemes were abandoned, ensuring the same number of schemes at the end of every generation. The children schemes would be considered as the parent schemes in the next generation. Finally, if the program was terminated, the schemes with maximum energy generated would be regarded as the most optimised and the best results for that GA model run.

In this GA model, two termination criteria were defined to stop the model running to infinity, namely ‘Another iteration’ and ‘Target’, as shown in Figure 3. The former was used to limit the generation increase and the latter was regarded as the ideal energy generation scheme.

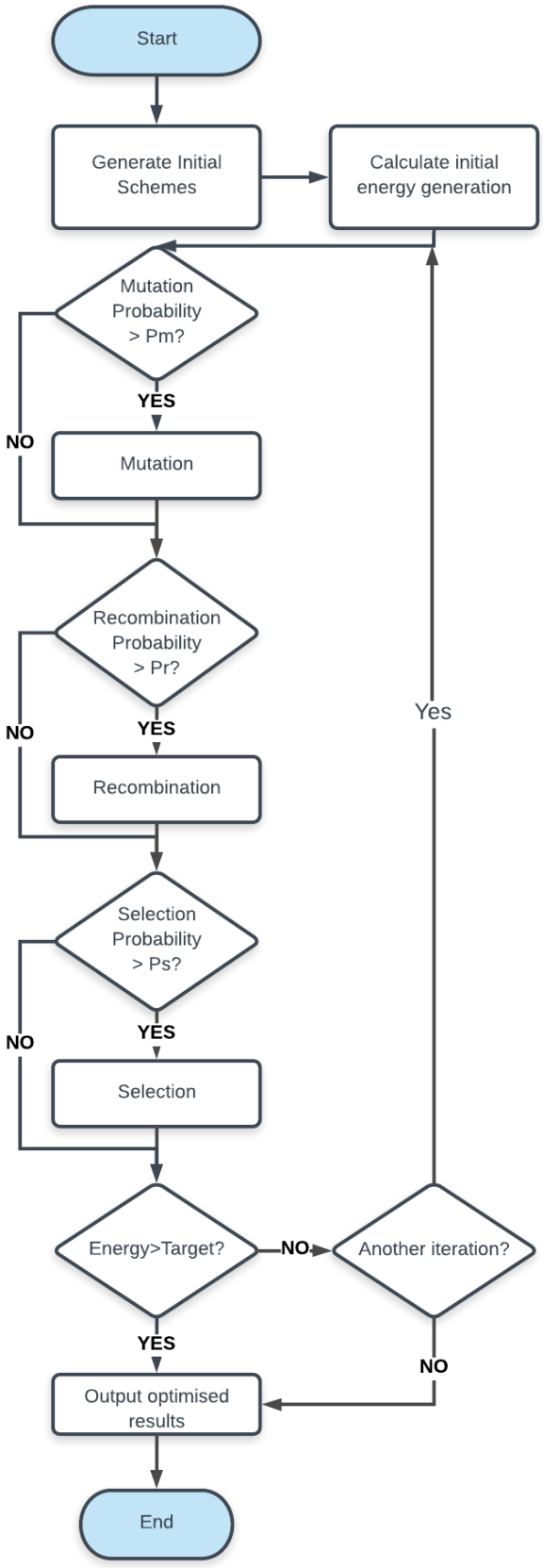

Fig.3. Flow-chart of the GA model used for Tidal Range Scheme optimisation [18].

In this study, every operational scheme included decision variables. The constants represented the number of turbines, i.e., NumTB, and sluice area capacity, i.e., STPC. The vectors represented the operation water heads for n successive half-tides, including starting, ending and pumping heads for flood and ebb tides, represented by $[H_{s,n}]$, $[H_{e,n}]$ and $[H_{p,n}]$, respectively. The number of vectors was reduced to two and the pumping head was omitted if pumping was not included in the model.

The GA model was developed based on the Sequential Mutation Method (SMM) and Ring Recombination Method (RRM). In each generation using SMM only one half-tide was selected from all of the half-tides and mutation was applied to all of the parameters for this half-tide. The selections of half-tides in SMM were in a sequential order, which progressed one step further in the next generation. After running the model for n generations, in the $(n+1)^{th}$ generation then mutation started from the 1st generation and this procedure then continued. The mutated parameter followed a normal distribution, with an assumed variance of 0.1. This representation was based on the nature of evolutionary processes and ensured that the genes from the children with mutated genes kept a certain relationship with the genes from their parents. In RRM, two schemes were selected for recombination, and then the starting point (i or j) and length (L) for recombination were generated randomly. The new children, i.e., schemes, were then generated by exchanging information from the parents, as shown in Figure 4. It should be noted that there was no limit to the magnitudes of L, considering the circular presentation of the data [20, 36, 38].

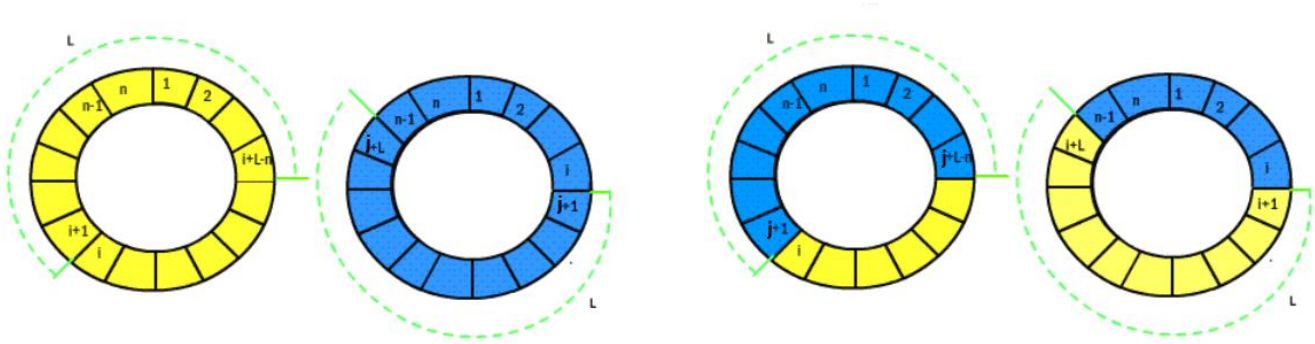

Fig.4. Ring Recombination Methods (RRM) illustration: (a) before RRM; and (b) after RRM.

4.3. Initial schemes generation and parameter setting

An individual with genes in the GA was replaced by the operation scenarios during every half-tide, as well as the values of NumTB and STPC. The range of starting heads (H_s) was assumed to be between 2.0 m and 8.0 m and the range of ending heads (H_e) was between 0.5 m and 4.5 m, ensuring a comprehensive search space for the operation heads. The range of pump heads (H_p) varied from 0 m to 4.0 m. To avoid the need for flood mitigation and modifications to the caissons, the water level after pumping was limited by the Highest Astronomical Tide (HAT) and the Lowest Astronomical Tide (LAT), which were recorded as being 5.98 m and -5.68 m, respectively. The number of turbines (NumTB) varied from 75 to 175 and the sluice capacity (STPC) varied from 0 to 8 m^2MW^{-1}, ensuring a relatively reasonable and cost-effective scheme. It should be noted that in the GA model the operation heads could be variables for each half-tide if flexible schemes were adopted or could be kept constant for non-flexible schemes, which affected the number of variables being optimised. However, the NumTB and STPC values were considered to be constant for each scheme, with the reason being that the number of turbines and sluicing area could not be changed once the project had been constructed.

More attention was paid to the convergence of the results in this study, rather than focusing on the control parameters in the GA model, and therefore P_m, P_r and P_s were set to be 0.5, 0.5 and 1, respectively. Moreover, the

terminal criterion of 'Target' was infinity and 'Another iteration' was 5000, allowing a sufficient number of iterations to achieve convergence and, in the meantime, guarantee an affordable run time on a High-Performance Computer (HPC). It was decided to allow 1000 initial solutions to be generated randomly, to ensure diversity of the population [35].

4.4. Fitness function

The 0-D model was set up using a backward-difference numerical formulation, based on solving the continuity (or mass conservation) equation. The water levels outside the impoundment Z_{up}^{i+1} at the $(i+1)^{th}$ time step were calculated using the upstream and downstream water levels at the previous time step, as follows:

$$Z_{up}^{i+1} = Z_{up}^{i} + \frac{Q(H)+Q_{in}}{A(t)}\Delta t \quad (1)$$

where Q_{in} is the inflow/outflow to the impoundment through sources/sinks, rather than through the TRS, e.g., a river or outflows (m^3/s); $A(t)$ is the wetted plan surface area of the impoundment (m^2) at time t and $Q(H)$ is the discharge through the turbines and sluices (m^3/s) [10]. The discharge through a turbine and the corresponding energy generated were calculated based on the head difference across the turbine using a double regulated hill chart [41] and the flow through a sluice gate (Q) was obtained using an orifice equation, as follows [42, 43]:

$$Q = C_d A_s \sqrt{2gH} \quad (2)$$

where C_d is the discharge coefficient which was assumed to be 1 in this study [44]; g is gravitational acceleration (m/s^2); A_s is the sluice gate area (m^2) and $H = Z_{up}^{i} - Z_{dn}^{i}$ (m).

The power used for pumping, namely P_{input}, was calculated based on the values reported for the pumping efficiency when the bulb turbines were used as pumps [27] giving:

$$P_{input} = \eta_p \times P_{potential} \quad (3)$$
$$P_{potential} = gH \times \rho Q(H) \quad (4)$$

where η_p is the pump efficiency; P_{input} denotes the consumed power used during the pumping phase (MW); $P_{potential}$ represents the potential power output (MW) in pumping, which was calculated based on gH and the fluid mass flow rate ($m^3\ s^{-1}$), i.e., given as $\rho gQ(H)$.

The total installed capacity of the scheme is equal to the number of turbines (NumTB), multiplied by the Installed Capacity of each turbine (IC) [2, 45]. Turbines with a diameter of 7.2 m and an Installed Capacity of 20 MW were used in this study. The sluice area (A_s) was optimised, based on the Sluice To Power (STPC) function, which expresses the ratio of the sluice area to the total installed capacity of the scheme, as given by:

$$A_s = NumTB \times IC \times STPC \quad (5)$$

STPC was used for optimisation of the sluicing area in order to make various scenarios of one scheme with different installed capacities or different schemes more comparable. The water levels series of tides at the downstream cross-section of WSL was generated from the validated DIVAST-2DU model without any structures, and then used in the 0-D model as the input tidal water levels. The DIVAST-2DU model is discussed in section 5.1,

Optimisation of a TRS for a year is computationally expensive and an approach often used to save computational time during optimisation is to use a typical spring-neap tidal cycle [7, 16] and extrapolate the generation over a year, to calculate the annual energy generated. The typical spring-neap cycle needs to be close to an average cycle over the year, otherwise the extrapolated predicted energy generated will be either an over or underestimation of the real value, thereby being problematic for developers. In order to find a typical annual mean spring-neap cycle, energy generation for all tidal cycles over the target year, 2012 in this study, was first calculated and a cycle with the closest generation to the average spring-neap cycle generation was selected as the typical spring-neap cycle. To identify the typical cycle, the initial number of turbines and sluice gate areas were required. These preliminary values were selected using other TRS proposals as an example and were optimised through this study. A combination of turbine numbers (increasing from 75 to 125 with 25 increments) and sluice gates (STPC of 0, 2, and 4 m^2MW^{-1}) were used, with non-flexible operating heads over the target year. The operation heads used were based on a comparison of the area with similar projects and are shown in Figure 5. As shown, the most efficient scheme had a starting head of 3.5 m and an ending head of 2.0 m, resulting in a peak output of 4.946 TWh/yr when 100 turbines were used, with a sluice capacity (STPC) of 4 m^2MW^{-1}.

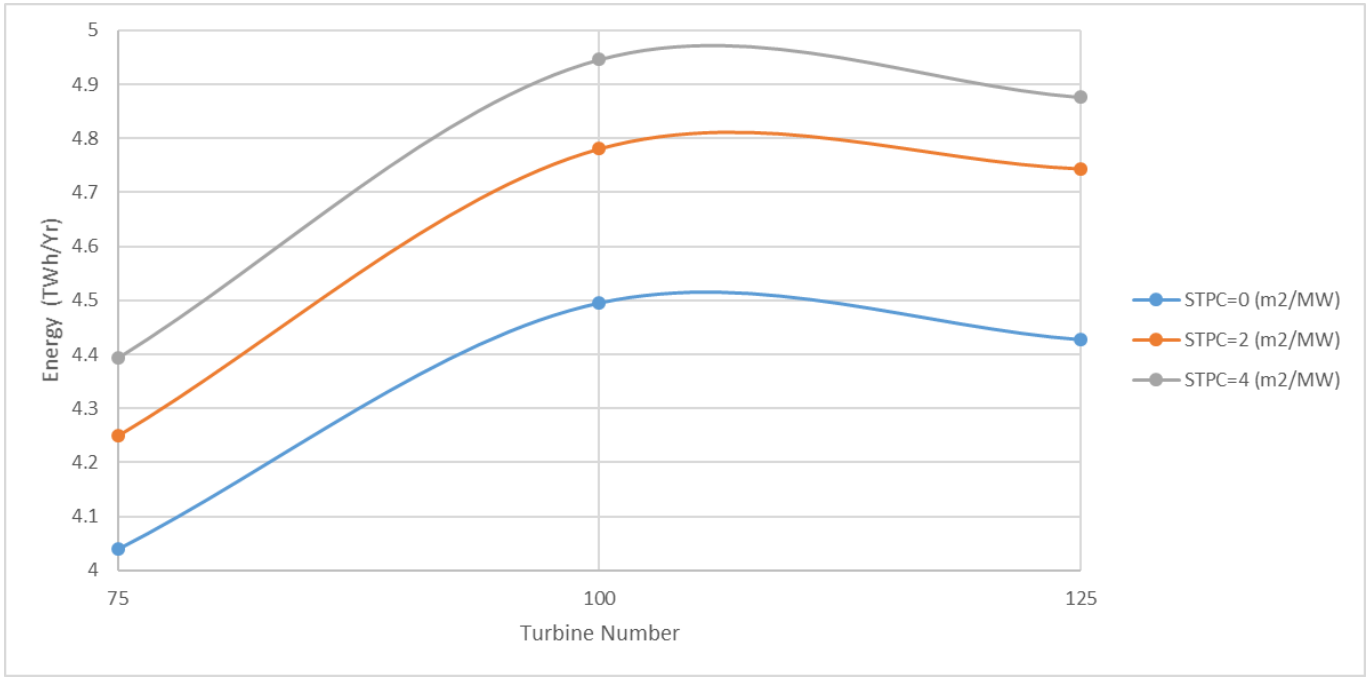

Fig.5. Energy generated with preliminary design parameters for non-flexible operation schemes, in which STPC represents the sluice capacity.

The tides in the target year were separated into 24 spring-neap tidal cycles. The average energy generated for all the cycles was approximately 200.8 GWh. The energy generated over various tidal cycles is shown in Figure 6. It can be seen that the 16th cycle, where the energy generated was 201.3 GWh, was the nearest to the average and hence this spring-neap typical cycle was selected as the baseline scenario in this study. This cycle extends from 5389.70 h to 5737.70 h from the start of the year. The extrapolation coefficient based on the ratio of the length of the year to the tidal cycle was 24.6.

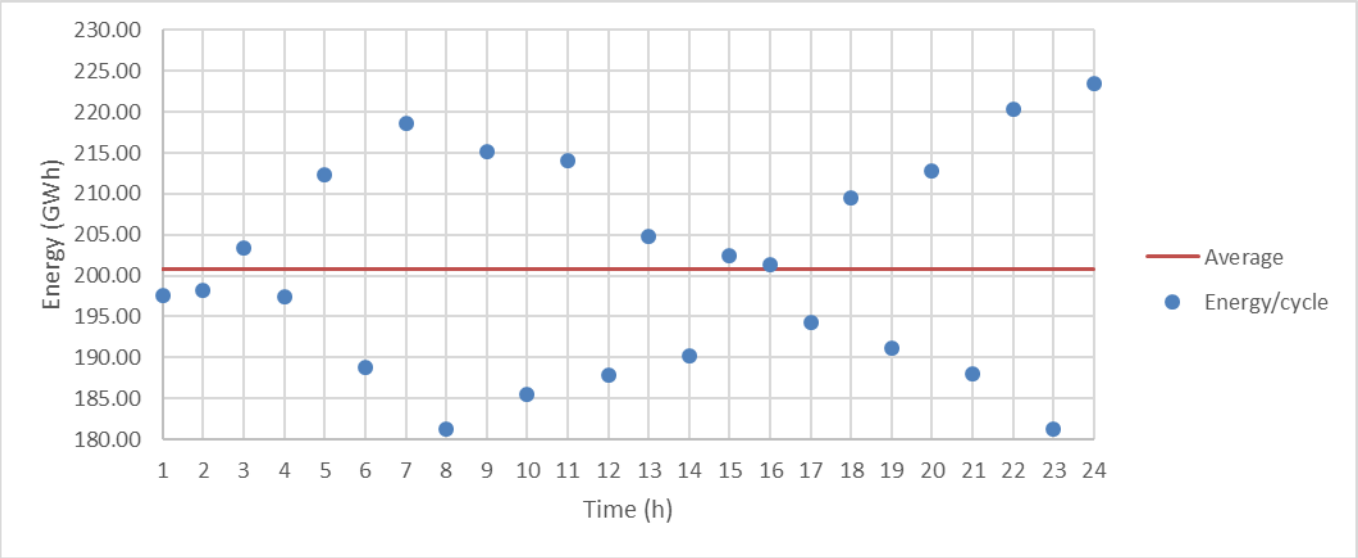

Fig.6. Energy generated per cycle from the 0-D model.

5. DIVAST 2D Model Details

5.1. 2-D modelling

Multi-dimensional models are routinely used to provide hydrodynamic simulations which can contribute valuable insight into the resource assessment of marine renewable energy schemes and device [46]. An in-house numerical model, namely DIVAST-2DU, has been widely used in modelling tidal renewable energy schemes and device and has also been used in this study [47, 48]. The governing equations in the DIVAST 2-DU model are the depth-integrated 3-D Reynolds Averaged Navier-Stokes (RANS) equations for impressible, unsteady turbulent flows. The 2-D model is built using a triangular unstructured mesh and with the primitive variable fields being water elevations (from Eq. 6) and velocities in the x and y directions (from Eqs. 7 and 8), respectively [49, 50].

$$\frac{\partial \xi}{\partial t} + \frac{\partial q_x}{\partial x} + \frac{\partial q_y}{\partial y} = 0 \tag{6}$$

$$\frac{\partial q_x}{\partial t} + \beta\left[\frac{\partial u q_x}{\partial x} + \frac{\partial v q_x}{\partial y}\right] = f q_y - gH\frac{\partial \xi}{\partial x} + \frac{\tau_{xw}}{\rho} - \frac{\tau_{xb}}{\rho} + \varepsilon\left[2\frac{\partial^2 q_x}{\partial x^2} + \frac{\partial^2 q_x}{\partial y^2} + \frac{\partial^2 q_y}{\partial x\,\partial y}\right] \tag{7}$$

$$\frac{\partial q_y}{\partial t} + \beta\left[\frac{\partial u q_y}{\partial x} + \frac{\partial v q_y}{\partial y}\right] = f q_x - gH\frac{\partial \xi}{\partial y} + \frac{\tau_{yw}}{\rho} - \frac{\tau_{yb}}{\rho} + \varepsilon\left[\frac{\partial^2 q_x}{\partial x^2} + 2\frac{\partial^2 q_x}{\partial y^2} + \frac{\partial^2 q_x}{\partial x\,\partial y}\right] \tag{8}$$

where ξ denotes the water elevation above (positive) UK ordnance datum (m); h represents the water depth below datum (m), with total water depth H being the sum of ξ and h; q_x, q_y are the discharges per unit width in the x, y directions, respectively ($m^2\ s^{-1}$); u and v are the velocity components in the x, y directions, respectively ($m\ s^{-1}$); β is the dimensionless momentum correction factor for a non-uniform vertical velocity profile; f represents the Coriolis parameter, which is caused by earth's rotation ($rad\ s^{-1}$); g is the gravitational acceleration($m\ s^{-2}$); τ_{xw} and τ_{yw} denote the components of the surface wind stress in the x, y directions respectively ($N\ m^{-2}$); τ_{xb} and τ_{yb} are bed shear stresses in the x, y directions, respectively; and ε is the depth-averaged eddy viscosity ($m^2\ s^{-1}$).

A domain decomposition technique was used to represent WSL in the DIVAST 2-DU model [51, 52]. This meant that the computational domain was divided into two sub-domains, one covering the area impounded by the lagoon and the other covering the rest of the domain outside of the lagoon [42, 52]. The sub-domains did not overlap, but were linked dynamically by the discharges flowing through the turbines and sluice gates [53]. The model was refined

in this study to operate flexibly, i.e., operating under different operation heads, in order to replicate exactly the same operational scheduling delivered by the GA model [20]. A smooth operation of WSL was guaranteed by coupling the operation of the turbines and sluice gates with a sinusoidal ramp function for opening and closing the device [51]. As this type of optimisation was carried out at an early stage in the feasibility and design of the scheme, the positioning of the sluice gates and turbines had not yet been finalised in the design and therefore they may subsequently be included in the deeper part of the impoundment wall, as shown in Figure 7. This positioning is expected to have a minimal impact on the predicted energy generated at the early stage of the feasibility design and which is the main purpose of this study. It should be noted that the same hill-chart in the GA model was used in this DIVAST 2-DU model, ensuring consistency in the discharge and energy output from the turbines used in both models. More details of the numerical solutions of the governing equations and implementation of TRSs in the model can be found in [11, 52].

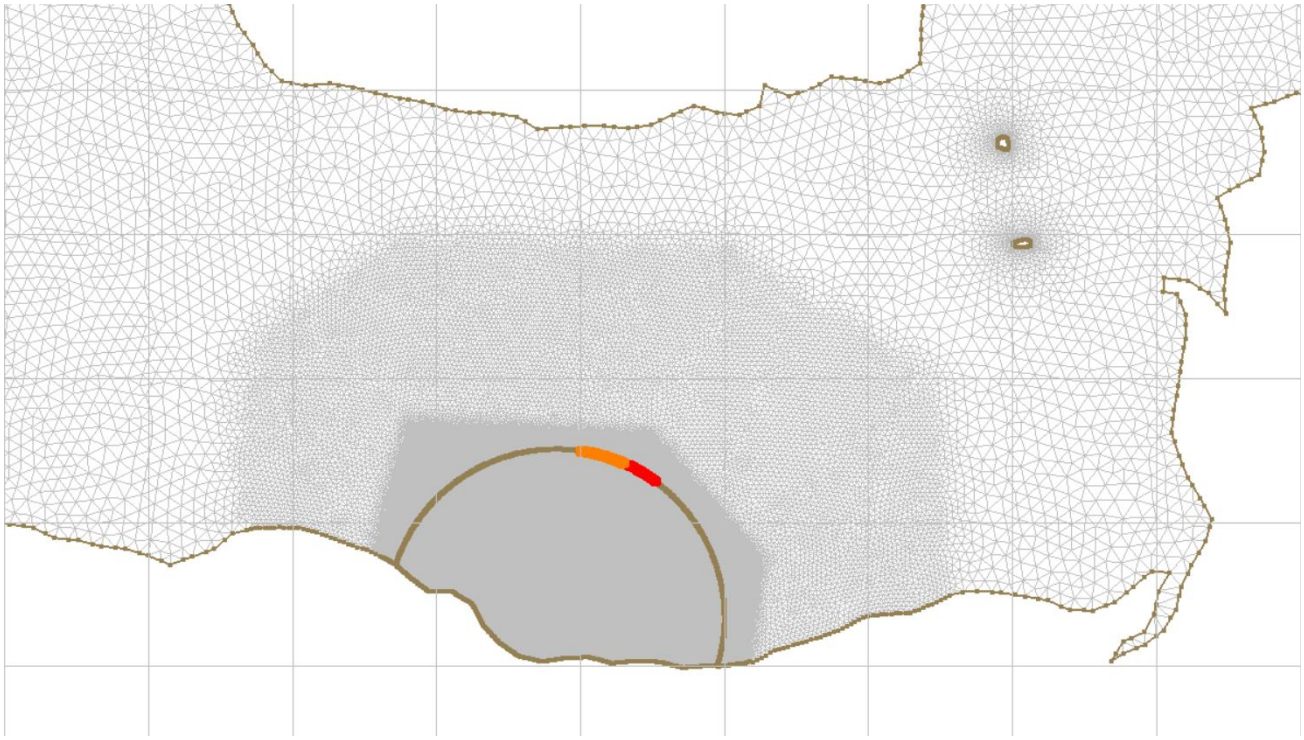

Fig.7. Sketch of grid refinement and deployment of turbines and sluice gates (Brown line is the wall boundary in the mesh, with the Orange line showing the turbines and the Red line showing the sluice gates).

5.2. 2-D Model set up

In this study, the DIVAST 2-DU model was set up to cover the Severn Estuary and Bristol Channel, encompassing an area of 5,805 km^2, thereby minimising any impact that the open boundary conditions might have on electricity generation by the lagoon, as shown in Figure 2. The bathymetry data were acquired from EDINA Digimap [54] and depths were interpolated at the centre of grid cells. The model domain was divided into 72,760 nodes and 143,203 unstructured triangular cells. The minimum grid size was approximately 50 m, in the vicinity of the scheme, thereby giving more accurate simulation of the hydrodynamics in the region of particular interest. For the baseline scenario with 100 turbines, two sub-domains were set-up inside and outside of the lagoon wall, and with lengths of approximately 1,200 m for the sluice gates and 1,800 m for the turbines, with a dividing structure wall of 200 m, as shown in Figure 7. The design of the turbines was taken from that used for the turbines outlined in the design of Swansea Bay Lagoon [18], with the length of each turbine encasement being 18 m. The tidal elevations for the seaward

boundary conditions were obtained from the National Oceanographic Centre [14]. The model, excluding the lagoon, has been widely calibrated and validated against observed data at different sites [16, 55]. It should be noted that the model has been validated for grid independency and the predicted results were not found accurate compared to the field data for this grid resolution [16]. A Manning's n roughness coefficient of 0.02 $s/m^{1/3}$ was used across the entire domain, with this value giving good agreement when calibrated against the field data. Water levels are always the most critical parameter for the operation of TRSs in terms of energy generation. Therefore comparisons of the model predictions and observed water levels during an average Spring-Neap tidal cycle in the vicinity of the WSL scheme are shown in Figure 8(a) and (b) for 4 spring tides at Hinkley and Ilfracombe, respectively, as shown in Figure 2, with more validation results being given in [16]. The Root Mean Squared Error (RMSE) for the tidal levels predicted by the model and observed values at Hinkley and Ilfracombe were 0.07 and 0.08 during the typical Spring-Neap tidal cycle, respectively. The Highest Water level (HW) was overestimated by about 0.3 m at Hinkley during spring tides, which meant that the input water level in the 0-D model may be overestimated with an overestimated energy prediction of less than 10% [16]. This level of error is consistent with other studies [47, 52, 56] and is considered to be acceptable for such studies [57].

It can also be seen that the differences between the model predictions and observed water levels at Hinkley Point gauge were greater at low water. Part of this difference, which is also observed at the Ilfracombe site, is thought to be due to discrepancies at the boundary. This is thought to be identified through differences in the local bathymetry near to the gauge site. This is further confirmed by achieving good comparison between the model predictions and the ADCP results as reported in [16]. These small discrepancies, which are typically 0.4 m of Lowest Water (LW) at Hinkley Point gauge, need to be studied further, however, they do not significantly affect the main objectives of this study.

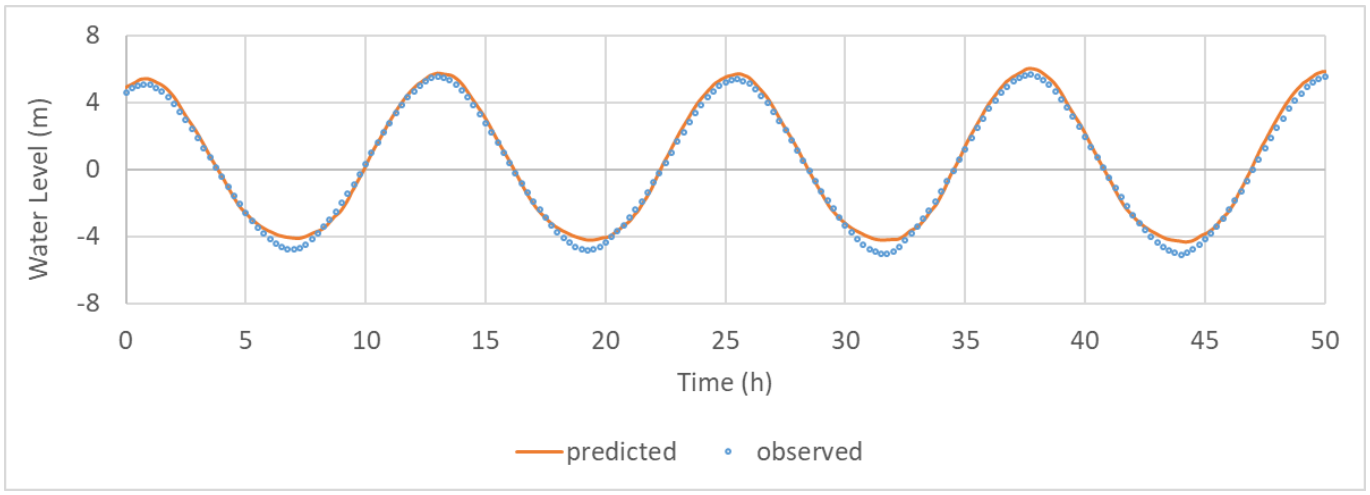

(a)

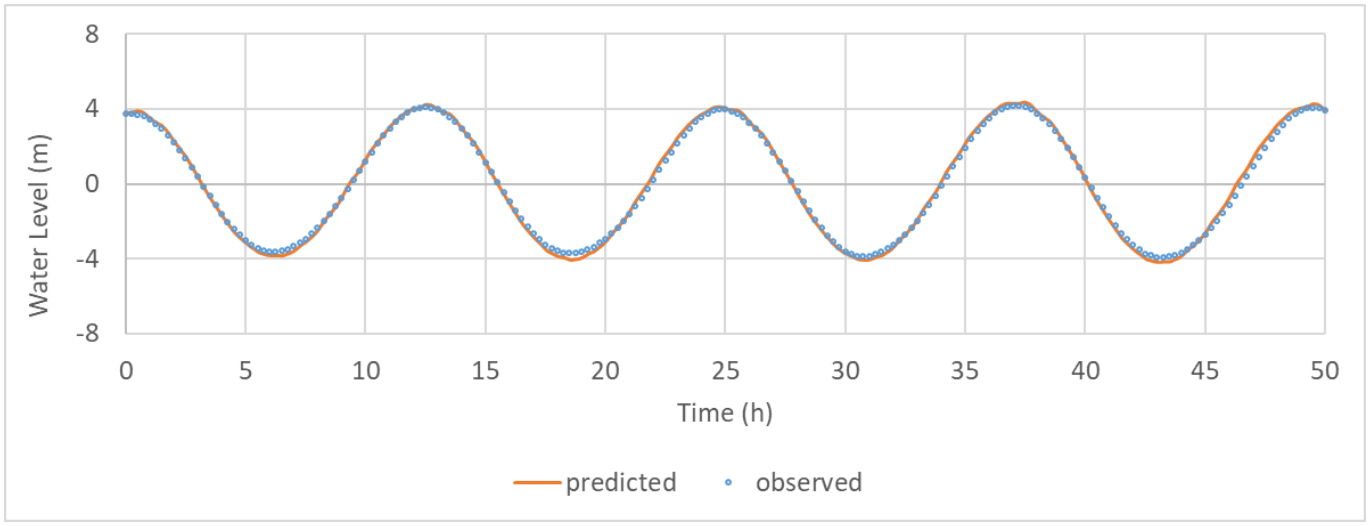

(b)

Fig.8. Typical comparison of observed and predicted water levels at: (a) Hinkley and (b) Ilfracombe.

6. Optimisation of West Somerset Lagoon Operation

6.1. Optimisation using the Grid Search (GS)model

The grid search model covered the entire solution domain and examined each possible scenario in order to find the optimum solution. As for the GA model, every operational scheme was encoded with two constant values in the GS model, namely NumTB and STPC, and two vectors, namely $[H_{s,n}]$ and $[H_{e,n}]$, representing the operation water heads for n successive tides. In considering the range of feasible operation heads of TRSs [16], the range of starting heads varied from 2.0 m to 8.0 m, in 0.1 m increments, and ending heads covering a range from 0.5 m to 4.5 m, also in increments of 0.1 m . NumTB was varied from 75 to 175, in increments of 5, and STPC varied from 4 to 8 m^2 MW^{-1}, with an increment of 1, making sure that it can reflect the trend of electricity generation with an affordable computational cost.

The maximum energy generated with different NumTB and STPC values over the representative period using the GS model, with non-flexible operation schemes, is shown in Figure 9. The maximum energy over the simulation period was achieved using 140 turbines, a sluice gate capacity of 8, a starting head of 5.5 m and an ending head of 2 m. An improvement of more than 25% of the energy generated was achieved for this case, in comparison with the baseline scenario shown in Figure 5 with NumTB and STPC values of 100 and 4 m^2MW^{-1}, respectively. It can be seen that with the turbine numbers increasing, the energy predicted first increases and then decreases moderately, with the peak value occurring when the number of turbines was between 140 and 150. The energy generated also generally increased with an increase in the sluice gate capacity. However, it is noteworthy that the energy generated rose slightly when the number of turbines exceeded approximately 125. TEES advised that this is unlikely to make the scenarios with more than 125 turbines less cost-effective because of the increasing capital cost with only a diminishing increase in energy. Since there are different ways in which the impoundment wall could be built, along with the turbine and sluice gate housings, and also that the turbines are not standard and are commercially sensitive, the cost was not considered in this paper. Also, around 5% of extra energy could be obtained using triple regulated turbines, but losses will inevitably arise due to turbines and sluice gates being out of operation for maintenance and energy losses in

connection to the grid. Hence, the most efficient scenario with the predicted maximum energy generated is shown in Table 1, with 125 turbines being utilised and a capacity factor of about 29%.

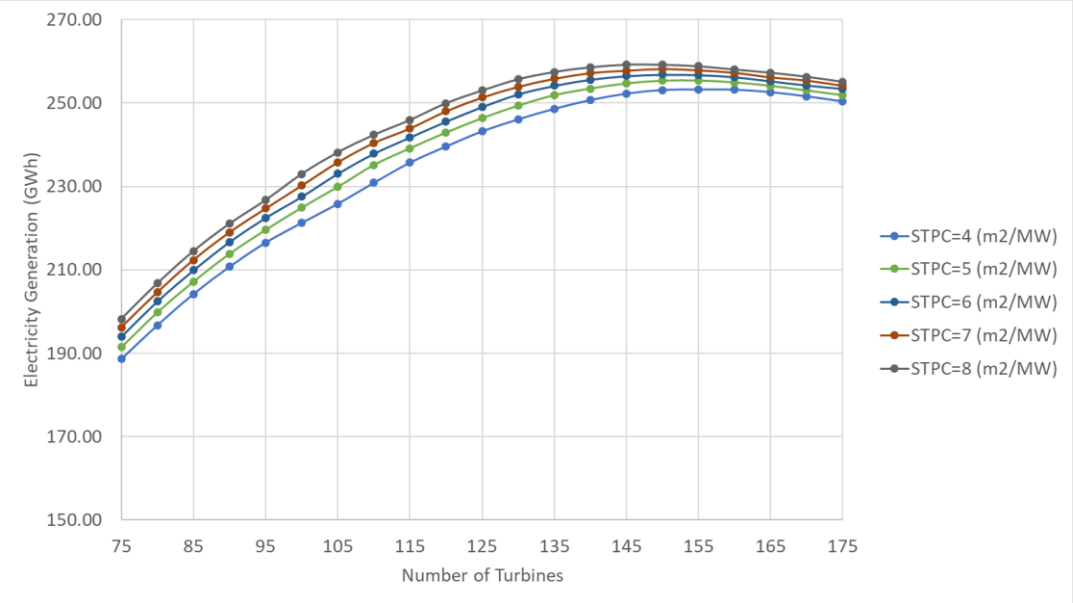

Fig.9. Energy generated for a range of turbines numbers and sluice capacities, for non-flexible schedules.

Table 1

Comparison of non-flexible optimisation scenarios.

	STPC (m^2 MW^{-1})	NumTB	Sluice Area(m^2)	H_{end}	H_{st}	Energy (GWh)*	Increase(%)	Capacity Factor (%)
Baseline	4	100	8000	2	3.5	201.3	-	28.92
GS	8	125	20000	2.5	4.9	253.4	25.87	29.12
GA	8	125	20000	2.5	5.0	252.6	25.50	29.04

* The extrapolation coefficient of 24.6 should be used to convert the energy from the average Spring-Neap cycle to annual generation.

As the best approach to optimise the operation of TRSs using the GS method was found to be obtained by simulating Every Half-tide and Next (EHN) [16], then this approach was adopted hereinafter for all studies. Figure 10 shows two idealised tides which were decomposed into their smallest operational units, namely half-tides, to demonstrate the EHN approach. The energy was calculated for each two successive half-tides, such as half-tide A and B. The starting and ending heads for half-tide A, which produced the maximum energy generated during the period of half-tides A and B, were chosen as the optimum scenario for the half-tide A. This enabled the generation during the next tide to be considered, based on the water level inside the impoundment at the end of each operation cycle, and with this being the starting water level for the next operation period. This maximised the energy output over one operation period, irrespective of the next period potentially reducing the energy generated over the next period. Therefore, the next half tide was considered in selecting the optimal generation for each operation period. Similarly, the optimum operation period for all other half-tides were considered for the next two half tides, namely half tides B and C, in isolation and with the starting head within the impoundment being derived from the optimum generation for

half tide A. This process was then continued throughout the duration with regard to the operation of the scheme, as shown in the Figure 11.

The flexible head operation was implemented with the fitness function over 59 half tides, which corresponded to the situation of 60 starting heads and 40 ending heads between each tide and the next half tide, 50 turbine numbers and 5 sluice gate capacity numbers, and with a time step of 1 minute. The optimisation of this flexible operation schedule using the GS method required approximately 430 hours of simulation time for the representative period, as shown in Table 2. This simulation time would be much longer when pumping is considered and the simulation covers more than a representative tidal cycle. This re-emphasises the significance of needing to reduce the model run time and improving the efficiency in the design of TRSs and hence the need to adopt more advanced algorithms, such as the GA for multiple variable optimisation.

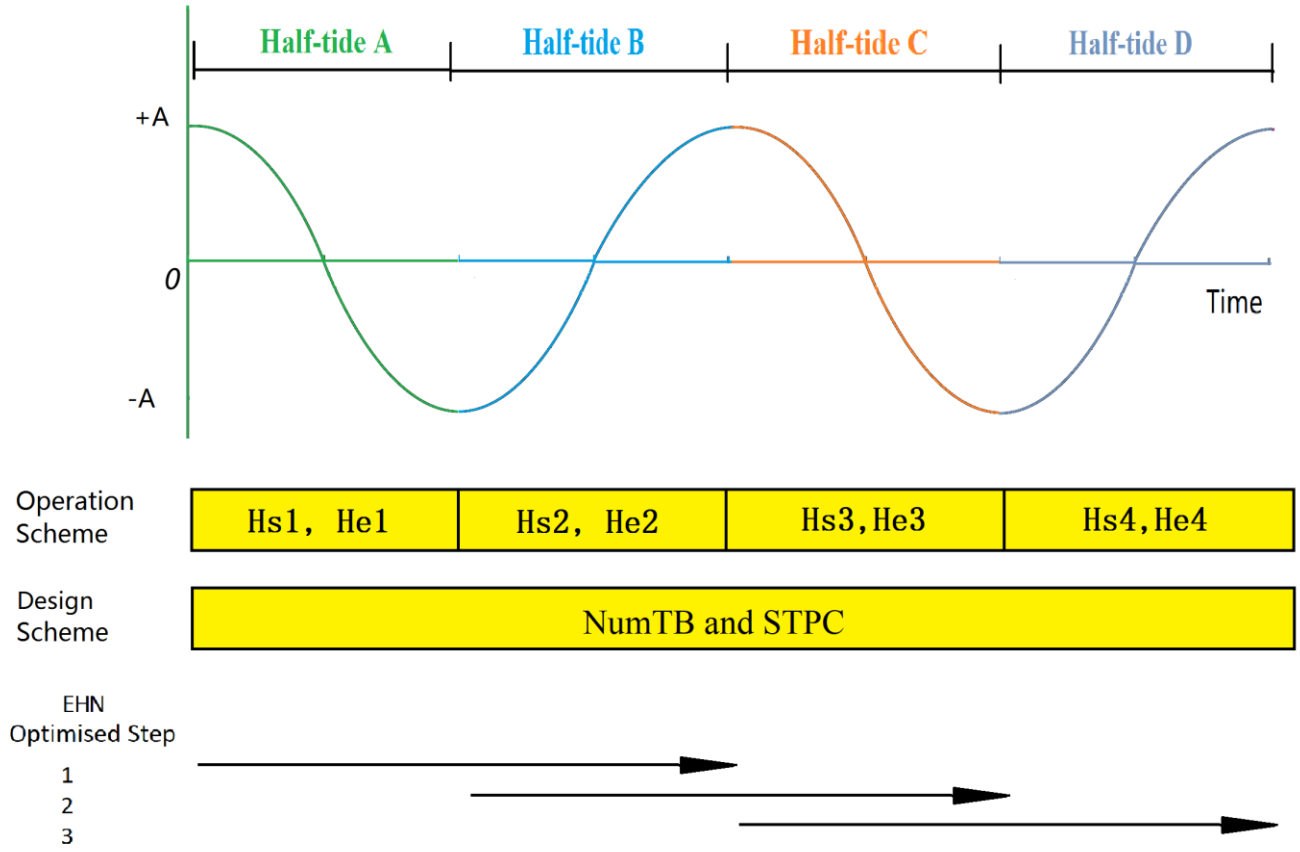

Fig.10. Schematic illustration of EHN (Every Half-tide and Next) optimisation methodology [16].

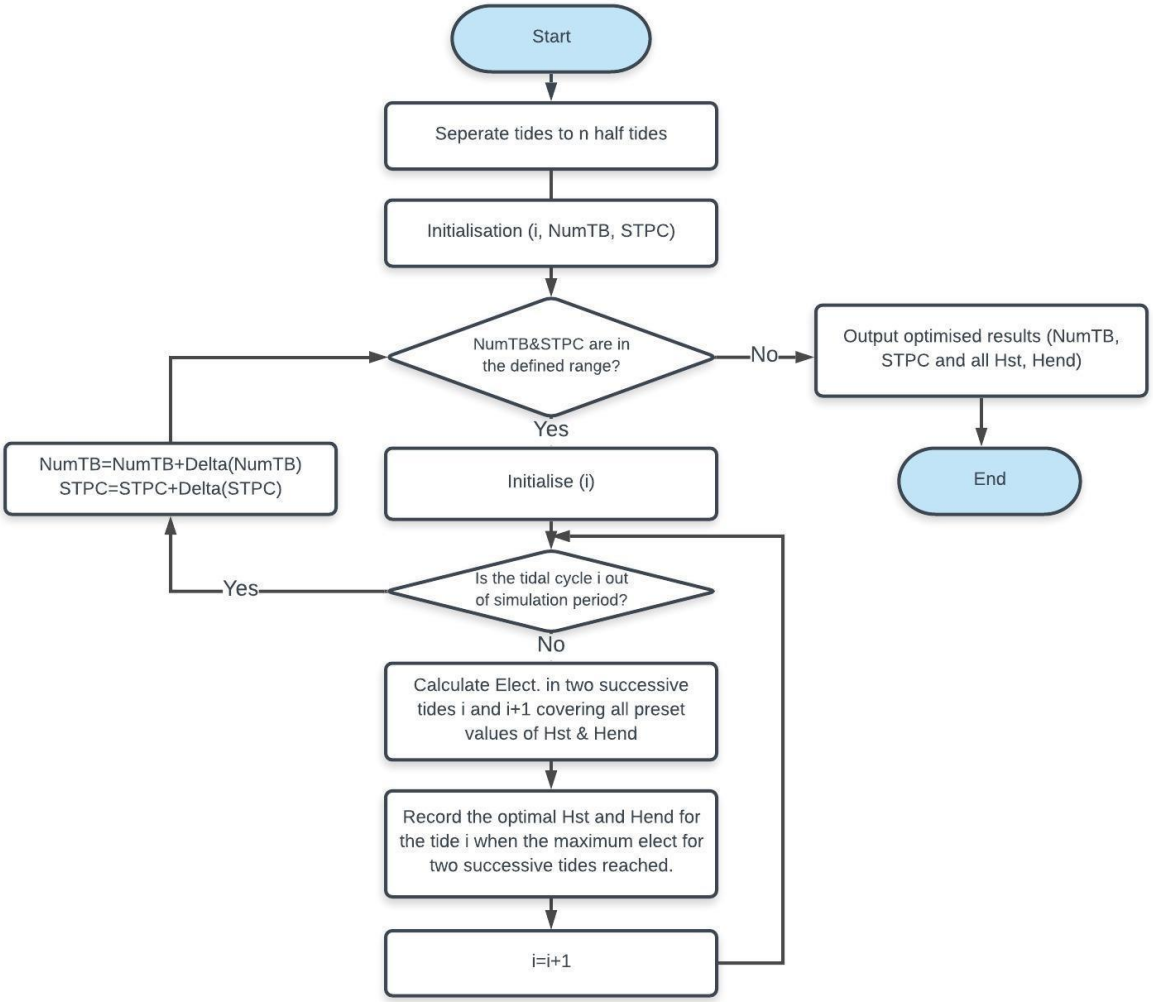

Fig.11. Flow-chart of the Grid Search model.

6.2. Optimisation using the GA model

If the non-flexible operation scheme is adopted in the GA model, then the most optimised scenario was obtained with an energy production of 252.6 GWh when H_s was 5.0 m and H_e was 2.5 m and with the number of turbines being 125 and the sluice gate capacity being 8, which equates to a sluicing area of 20,000 m^2 excluding the area of the turbine passage. The optimisation of multiple variables, including turbine numbers and sluice gates, with a non-flexible operation schedule yields an increase of more than 25% of energy generation, compared to the baseline scenario which applied NumTB of 100 and STPC of 4 m^2MW^{-1} with a H_s value of 3.5 m and H_e of 2.0 m, as outlined in Section 4.4. The estimated energy generated could be further improved by approximately 10% if flexible operation was adopted, which is in line with the findings by Xue et al. [16] and Angeloudis et al. [7]. The addition of pumping results in a further net energy yield of up to 291.1 GWh, with a capacity factor of approximately 33.46%, corresponding to a further improvement of electricity generation of about 10% compared to the scenarios without pumping. This net energy yield was calculated after deducting the energy used for pumping in determining the pumping efficiency [16]. The capability to pump is desirable for TRSs as it also provides flexibility and storage capability and reduces the hydro-environmental impacts. Therefore, it is essential that the pumping performance of TESs is studied further in the future. These scenario results and improvements in the energy generated are presented in Table 2. As can be seen in Table 2, the optimisation through the GA model produced very similar quantities of

energy for both the non-flexible and flexible operation schemes [16]. However, the simulation time for the GA model was approximately 95% less simulation time in comparison with the GS method for flexible operation. This significant reduction in the simulation time is particularly important in the early stages of design, where a large number of scenarios for different sizes and turbine/sluice gate combinations would be considered and expected to facilitate the development of TRSs by providing stakeholders with a more efficient tool to consider a wide range of scenarios. It should be noted that the cost of the GA model in Table 2 can be influenced by a variety of factors [22], such as the iteration time (5000 in this study), initial operation solutions (1000 in this study) as well as the performance of the HPC facilities, which is worthy of further consideration in future studies to acquire a higher efficiency of optimisation using this GA model.

Table 2 Comparison of optimisation scenarios.

Scenario			Energy (GWhr)		Change to baseline (%)		Difference between 0-D and 2-D (%)	Simulation time (hr)
			0-D model	2-D model	0-D model	2-D model		
No pumping	baseline [1]		201.3	183.5	-	-	-8.84	4
	GS	non-flexible [2]	253.4	226.3	25.87	23.33	-10.69	22.5
		flexible	271.7	245.4	34.96	33.74	-9.67	430
	GA	non-flexible [2]	252.6	225.9	25.50	23.14	-10.56	22
		flexible	270.0	244.0	34.15	33.00	-9.63	24
pumping	GA	flexible	291.1	266.5	44.64	45.28	-8.45	31

[1] Details of baseline scenario denotes the scheme with operation heads of 3.5m H_{st} and 2m H_{end} when using 100 turbines and a sluicing area of 8000 m^2, as shown in Table 1.

[2] Non-flexible operation schemes are represented using constant operation heads throughout the simulation period.

The detailed operation heads, water levels inside and outside of the impoundment and energy output during 5 neap tides, without and with pumping, are illustrated in Figures 12 and 13, respectively. These graphs highlight the variability in the energy output for the various operational heads, and with different half tides demonstrating the importance of considering variable heads, despite the higher computational time. It should be noted that, as expected, the energy output during neap tides is still lower than that for spring tides, even with the flexible operation schemes.

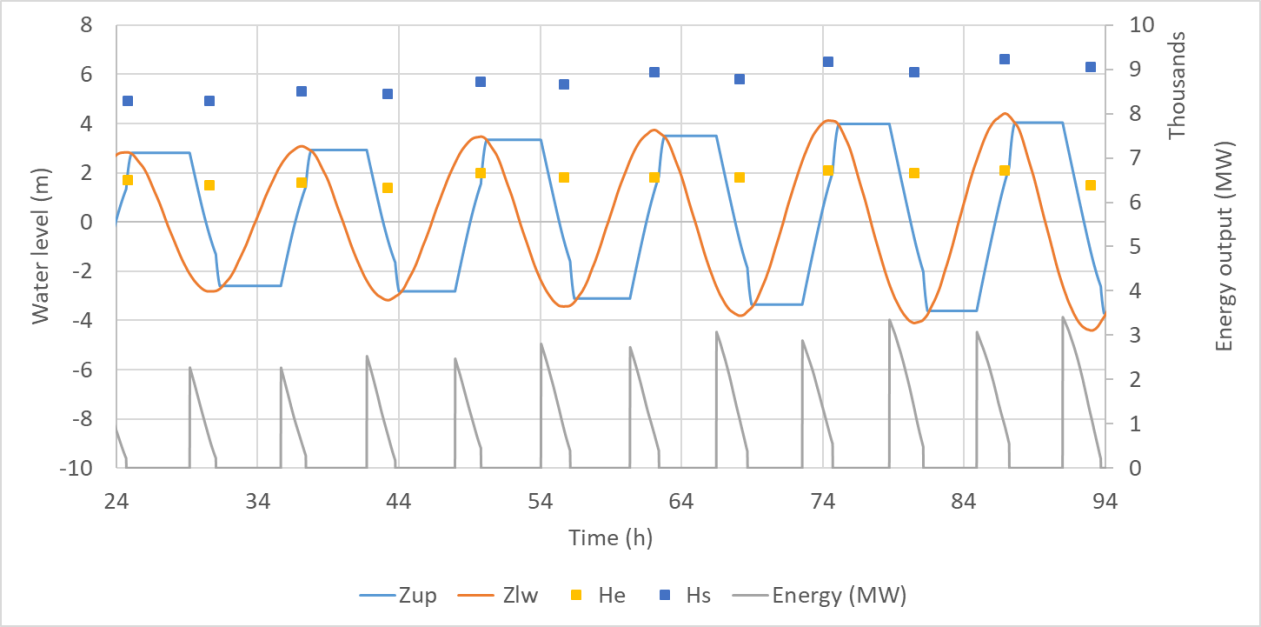

Fig.12. Predictions from the GA model of operation heads, water elevations inside and outside of the lagoon and energy output for 5 neap tides, in which the 'Zup' and 'Zlw' denote the water levels inside and outside of the lagoon, respectively, 'Hs' and 'He' represent the optimum operation heads when the generating phase starts and ends, respectively, and 'Energy' describes the energy output.

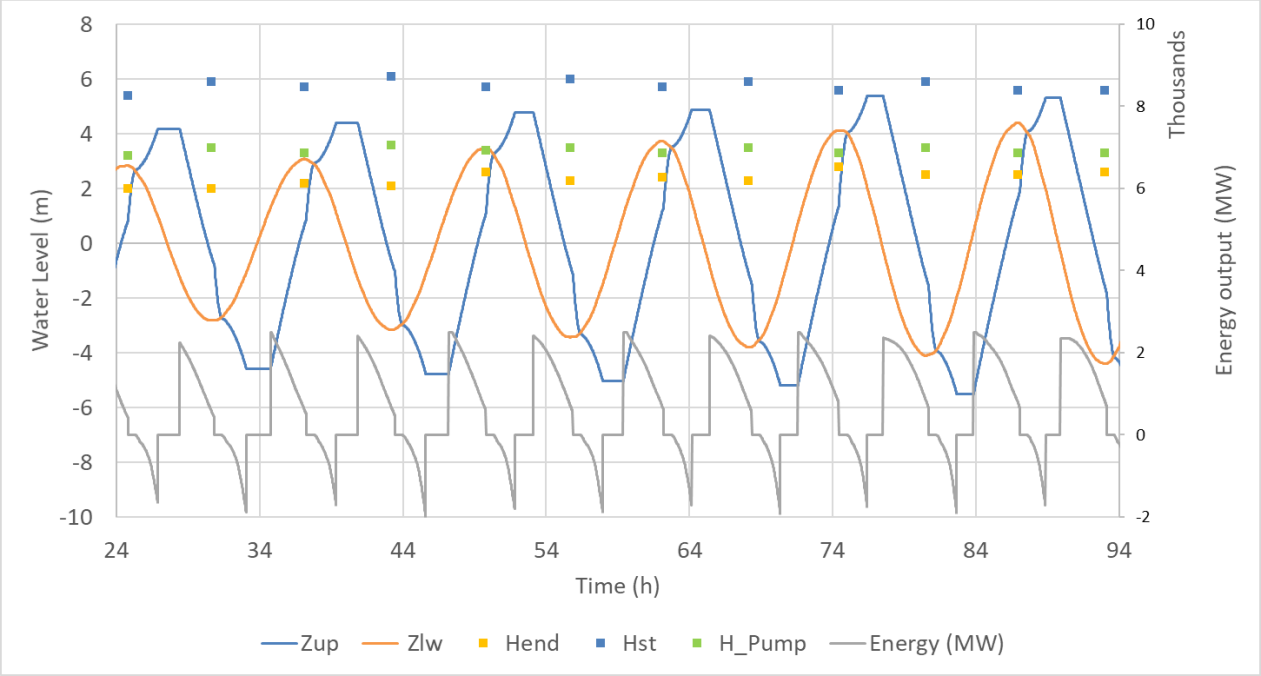

Fig.13. Predictions from the GA model of operation heads, water levels inside and outside of the lagoon and energy output with pumping for 5 neap tides, with the notation as for Figure 12.

6.3. Validating the operation schemes

The validity of the operational scheduling derived from the GA model was confirmed using the 2D model. This was undertaken mainly to ensure that the simplifications used in the 0-D fitness function were not leading to unrealistic operations. Figures 14 and 15 show the complex velocity fields for the ebb and flood tides, during sluicing and generating modes and for the baseline scenario, respectively. During the sluicing mode, with the turbines and sluice gates opening, the velocity was generally less than 2.0 m/s downstream of the sluice gates and 1.0 m/s downstream of

the turbines. During the generating mode, as the water flowed through the turbines and with all the sluice gates closed, the velocity in the vicinity of the turbines could reach magnitudes of up to 2.5 m/s. In the later stages of design, it is therefore important to investigate the positioning of the turbines and sluice gates in more detail to establish their hydro-environmental impact on tides, water quality, sediment transport, ecology and fish migration, as well as safety for navigation and recreational activity. The deployment of WSL and other sources of uncertainties, including positioning of the turbines and sluice gates, storm surges and their impact on energy generation [58], as well as the hydro-environmental impacts of the scheme all require further investigation.

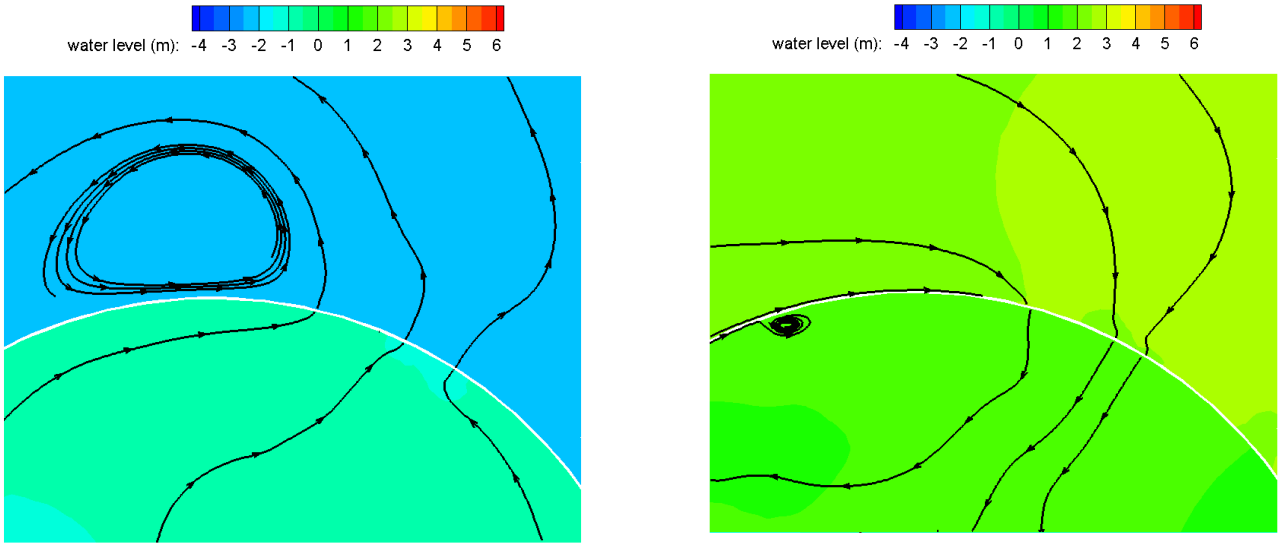

Fig.14. Water level and current streamlines in the 2-D model for: (a) ebb and (b) flood sluicing modes, respectively.

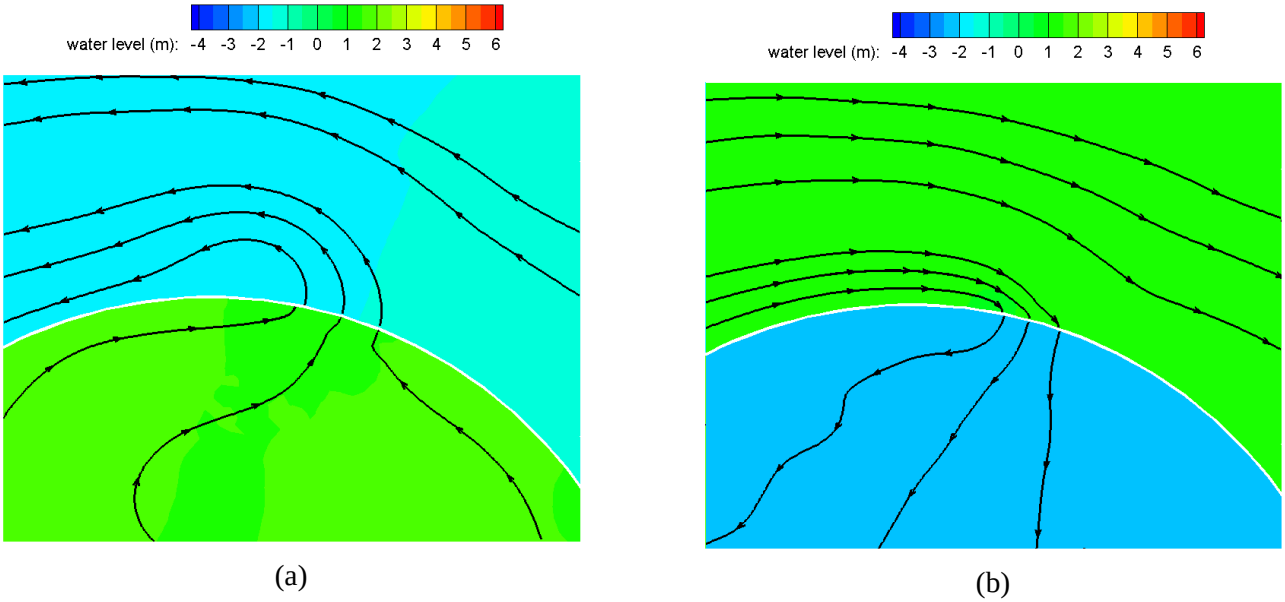

Fig.15. Water level and current streamlines in the 2-D model for: (a) ebb and (b) flood generating modes, respectively.

Since this study has mainly focused on the optimisation of various turbine and sluice gate operations, rather than investigating the hydro-environmental performance of a tidal range energy generation scheme, no extra momentum

source terms have been included across the impoundment wall to improve on the accuracy of the wake characteristics. The momentum source across the impoundment wall is expected to have little impact on the predicted energy generation as shown by Coz et al [13], but it would affect the wake characteristics and the local hydro-environmental features. The 2-D model predictions were firstly carried out for a variety of scenarios, as summarised in Table 2. The corresponding results revealed good agreement between the regression results for the water levels upstream and downstream, energy output, and the discharge through the turbines and sluices gates when the predicted results from the 0-D and 2-D models were compared. The total energy generated during a typical tidal cycle, as predicted by the 0-D model, was approximately 10% different in value to that predicted using the 2-D model, as shown in Table 2. These values are consistent with the values reported in the literature [16, 59] and need to be taken into account in the feasibility stage. Typical comparisons for the 0-D and 2-D model predictions are illustrated in Figure 16. Table 2 shows the energy generation under flexible operation for the optimised number of turbines and sluice gates, leading to an increase of approximately 25% and 10% compared with the baseline scenario and optimised for the non-flexible head scenario, respectively. This validates the feasibility of the operational schemes produced using the GA model and hence confirms the performance of the GA model in first designing TRSs by optimising the number of turbines and sluice gates and the operation schedule.

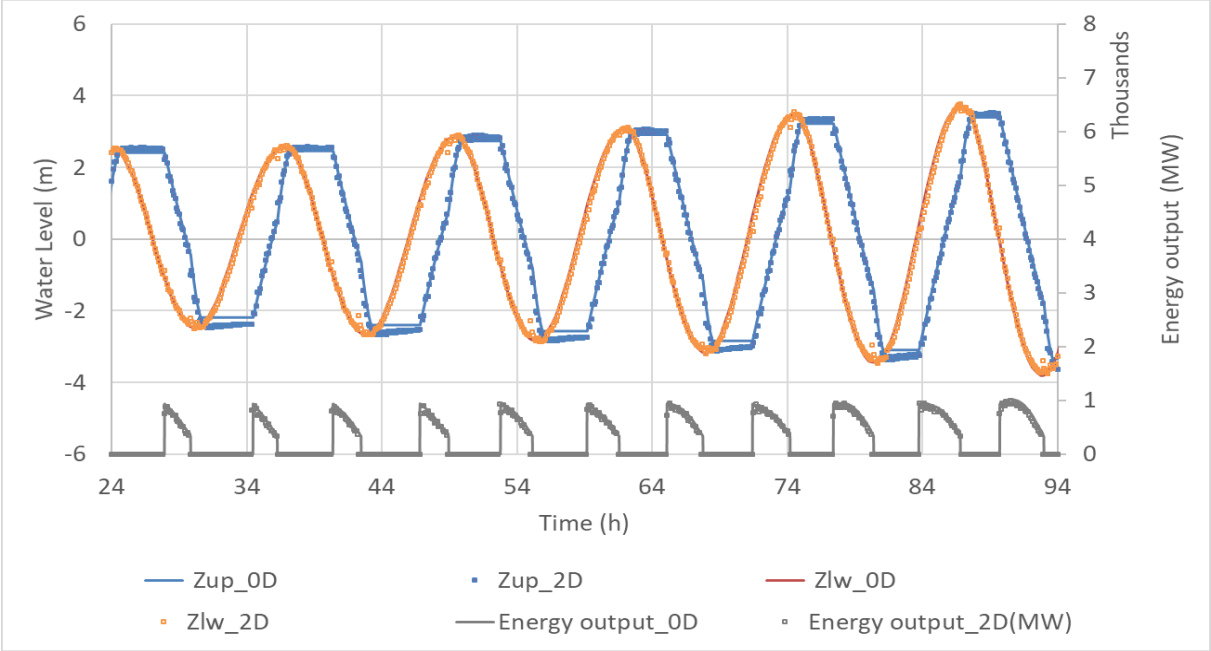

(a)

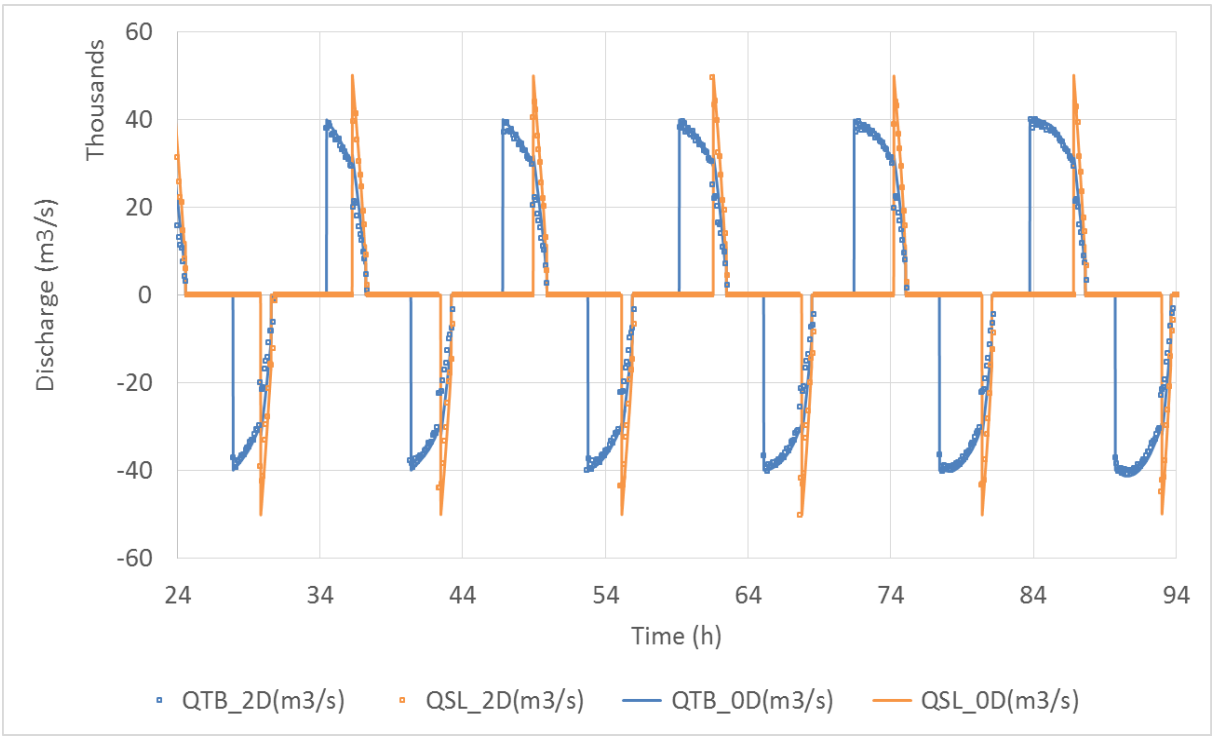

(b)

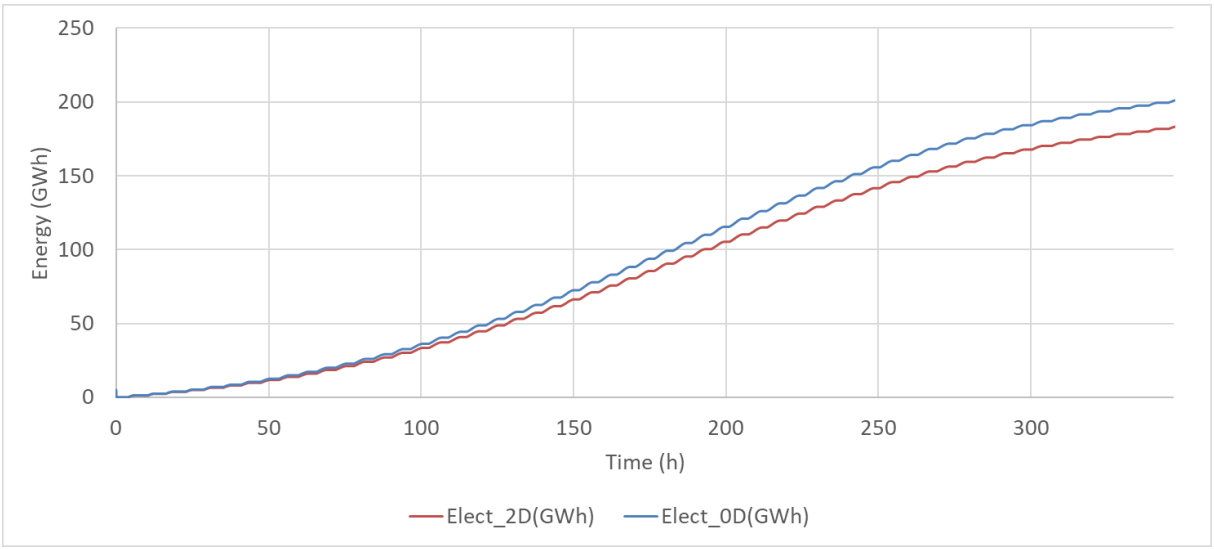

(c)

Fig.16. 2-D and 0-D model comparisons between: (a) water level and energy output during 5 neap tides; (b) discharge through the sluice gates and turbines during 5 neap tides (with flow into the lagoon shown as +ve); and (c) energy generated throughout a typical spring-neap cycle, in which the 'Zup' and 'Zlw' represent the upstream and downstream water levels, respectively, Energy denotes the energy generated, and 'QTB' and 'QSL' denote the discharge through the turbines and sluice gates, respectively.

7. Conclusions

The paper focuses on the development of a Genetic Algorithm model which can be used in the early stages of the design of any Tidal Range Schemes around the world to establish the optimal operating characteristics of the scheme for energy generation. The Genetic Algorithm model includes multiple variables related to the scheme, including

turbines numbers, sluicing areas and the operation schedule of the scheme, with the aim being to generate the maximum energy from the scheme. The model has been used to study the optimal design of a recently proposed Tidal Range Scheme (TRS) in the Bristol Channel, in the south west of the UK, called West Somerset Lagoon. The optimised scheme obtained using the Genetic Algorithm model provided a similar optimised scheme, in terms of the number of turbines, sluice area and total energy generated, as the widely used and more elaborate Grid Search model [16]. The developed Genetic Algorithm model reported herein reduced the computational time by approximately 95% in comparison with the Grid Search model.

The Genetic Algorithm model considered 1,000 different scheme configurations, generated randomly at the start and then evolved through mutation, recombination and selection, using specific probability parameters, and with the ideal outcome obtained or the maximum number of generations reached. A generalised 0-D model has been used as the fitness function, with the Sequential Mutation Method and the Ring Recombination Method being used for mutation and recombination.

The optimum initial design for the West Somerset Lagoon scheme was found to be 125 turbines, each of 7.2 m in diameter, and with a sluice area of 20,000 m^2. The optimised scheme, including a flexible operation design, using the Genetic Algorithm model, showed an increase of 25% and 10% in energy generation compared to the baseline scenario and the scenario with a fixed head operation. The performance of the model was validated by setting up a more sophisticated 2-D hydro-environmental model to simulate the operation of the scheme, based on the optimised Genetic Algorithm model design. Hence, the optimised energy generation reached 7.16 TWh/yr from the 0-D results and 6.56 Twh/yr from the 2-D model with the use of pumping. It was found that the differences between the Genetic Algorithm model and the 2-D model predictions were consistent with differences reported in the literature between 0-D and 2-D models, for impoundments of comparable size and shape. These findings confirm the performance and effectiveness of the Genetic Algorithm model in the preliminary design and feasibility of such tidal range schemes for the maximisation of electricity generation. However, one of the limitations of this Genetic Algorithm model is that it did not consider the effects of the hydrodynamics in the model, which could be improved through further case study applications worldwide. It is also worthy of further development of the Genetic Algorithm model for more goals, including: revenue optimisation, instead of only maximising the electricity generation, as undertaken in this study.

The Genetic Algorithm model reported herein has been shown to be significantly faster computationally than the Grid Search model for certain scenarios in applying the model to a tidal range energy generation scheme, namely the West Somerset Lagoon. However, although the model has been shown to be more efficient for this particular case study, the computational efficiency characteristics of the Genetic Algorithm model are generic and the same computational efficiencies would be expected for any tidal range energy generation study undertaken for any site world-wide.

ACKNOWLEDGMENTS

The first author Jingjing Xue would like to thank the China Scholarship Council (CSC) and Cardiff University for supporting this work. The authors are also grateful to the developer TEES, especially Directors Professor Chris Binnie FREng, FICE and David Kerr FICE for their constructive comments throughout the study.

References

[1] R. Baños, F. Manzano-Agugliaro, F. G. Montoya, C. Gil, A. Alcayde, and J. Gómez, "Optimization methods applied to renewable and sustainable energy: a review," Renewable and Sustainable Energy Reviews 2011;15(4);1753-66.

[2] S. Waters and G. Aggidis, "A world first: swansea bay tidal lagoon in review," Renewable and Sustainable Energy Reviews 2016;56;916-21.

[3] World Energy Council, World energy resources marine energy; 2016. <https://www.worldenergy.org/wp-content/uploads/2017/03/WEResources_Marine_2016.pdf>

[4] T. Güney, "Renewable energy, non-renewable energy and sustainable development," International Journal of Sustainable Development & World Ecology 2019;26(5);389-97.

[5] G. Rajgor, "Tidal developments power forward," Renewable Energy Focus 2016;17(4);147-9.

[6] S. Hinson. Tidal lagoons; 2018. <https://commonslibrary.parliament.uk/science/environment/tidal-lagoons/>
[7] A. Angeloudis, S. C. Kramer, A. Avdis, and M. D. Piggott, "Optimising tidal range power plant operation," Applied Energy 2018;212;680-90.
[8] S. P. Neill, A. Angeloudis, P. E. Robins, I. Walkington, S. L.Ward, and I. Masters, et al., "Tidal range energy resource and optimization – past perspectives and future challenges," Renewable Energy 2018;127;763-78.
[9] D. Prandle, "Simple theory for designing tidal power schemes," Advances in Water Resources 1984;7(1);21-7.
[10] A. Angeloudis, R. Ahmadian, R. A. Falconer, and B. Bockelmann-Evans, "Numerical model simulations for optimisation of tidal lagoon schemes," Applied Energy 2016;165;522-536.
[11] R. Ahmadian, R. A. Falconer, and B. Bockelmann-Evans, "Comparison of hydro-environmental impacts for ebb-only and two-way generation for a severn barrage," Computers & Geosciences 2014;7;11-9.
[12] R. A. Falconer, J. Xia, B. Lin, and R. Ahmadian, "The severn barrage and other tidal energy options: hydrodynamic and power output modeling," Science in China Series E: Technological Sciences 2009;52(11); 3413-24.
[13] N. Čož, R. Ahmadian, and R.A. Falconer, "Implementation of a full momentum conservative approach in modelling flow through tidal structures," Water 2019;11;1917.
[14] R. Ahmadian, J. Xue, R. A. Falconer, and N. Hanousek, "Optimisation of tidal range schemes," The 12th European Wave and Tidal Energy Conference, Ireland; 2017.
[15] N. Yates and B. Tatlock, "Optimising tidal lagoons," The 12th European Wave and Tidal Energy Conference, Ireland; 2017.
[16] J. Xue, R. Ahmadian, and R. A. Falconer, "Optimising the operation of tidal range schemes," Energies 2019;12(5);2870.
[17] F. Harcourt, A. Angeloudis, and M. D. Piggott, "Utilising the flexible generation potential of tidal range power plants to optimise economic value," Applied Energy 2019;237;873-84.
[18] J. Xue, R. Ahmadian, and O. Jones, "Genetic Algorithm in Tidal Range Schemes' Optimisation," Energy 2020;200;117496.
[19] A. P. Alves da Silva and P. J. Abrao, "Applications of evolutionary computation in electric power systems," Proceedings of the 2002 Congress on Evolutionary Computation, USA; 2002.
[20] B. Pavez-Lazo and J. Soto-Cartes, "A deterministic annular crossover genetic algorithm optimisation for the unit commitment problem," Expert Systems with Application 2011;38(6);6523-29.
[21] A. S. Tasan and M. Gen, "A genetic algorithm based approach to vehicle routing problem with simultaneous pick-up and deliveries," Computers & Industrial Engineering 2012;62(3);755-61.
[22] P. Liashchynskyi and P. Liashchynskyi, "Grid Search, Random Search, Genetic Algorithm: A Big Comparison for NAS," Mathematics, Computer Science 2019; arXiv:1912.06059v1.
[23] E. Kontoleontos and S. Weissenberger, "Annual energy production maximization for tidal power plants with evolutionary algorithms," International Journal of Fluid Machinery and Systems 2017;10(3);264-73.
[24] P. B. Leite Neto, O. R. Saavedra, and L. A. Souza Ribeiro, "Optimization of electricity generation of a tidal power plant with reservoir constraints," Renewable Energy 2015;81;11-20.
[25] A.Cornett, J.Cousineau, and I.Nistor, "Assessment of hydrodynamic impacts from tidal power lagoons in the Bay of Fundy," Energy 2013;1;33-54.
[26] A. Angeloudis, M. Piggott, S. Kramer, A. Avdis, D. Coles, and M. Christou, "Comparison of 0-D, 1-D and 2-D model capabilities for tidal range energy resource assessments," Proceedings of European Wave and Tidal Energy Conference 2017.
[27] N. Yates, I. Walkington, R. Burrows, and J. Wolf, "The energy gains realisable through pumping for tidal range energy schemes," Renewable Energy 2013;58;79-84.
[28] "Report of the Severn Barrage Committee," HMSO, 1933.
[29] R. Ahmadian, R. A. Falconer, and B. Lin, "Hydro-environmental modelling of proposed severn barrage, UK," Proceedings of the Institution of Civil Engineers - Energy 2010;163(3);107-17.
[30] C. Binnie, "Private Communication" 2019.
[31] L. Mackie; D. Coles; M. Piggott; A. Angeloudis. "The potential for tidal range energy systems to provide continuous power: a UK case study". Marine Science and Engineering 2020;8(10);780-803.
[32] J. H. Holland, "Adaptation in natural and artificial systems," 1975.
[33] S. Basu, A. Sarkar, K. Satheesan, and C. M. Kishtawal, "Predicting wave heights in the north Indian Ocean using genetic algorithm," Geophysical Research Letters 2005;32(17); L17608.
[34] D. E. Goldberg and J. H. Holland, "Genetic algorithms and machine learning," Machine Learning 1988;3(2);95-9.
[35] S. R. Ladd, "Genetic Algorithms in C++," 1995.
[36] M. B. Nia and Y. Alipouri, "Speeding up the genetic algorithm convergence using sequential mutation and circular gene methods," The 9th International Conference on Intelligent Systems Design and Applications, Italy; 2009.
[37] S. B. A. Bukhari, A. Ahmad, S. Auon Raza, and N. Siddique, "A ring crossover genetic algorithm for unit commitment problem," Turkish Journal of Electrical Engineering and Computer Sciences 2016;24;3862-76.
[38] R. Dulbecco and M. Vogt, "Evidence for a ring structure of polyoma virus DNA," Proceedings of the National Academy of Sciences of the United States of America 1963;50(2);236-43.
[39] R. Weil and J. Vinograd, "The cyclic helix and cyclic coil forms of polyoma viral DNA," Proceedings of the National Academy of Sciences 1963;50(4); 730.
[40] S. Loussaief and A. Abdelkrim, "Convolutional Neural Network Hyper-Parameters Optimization based on Genetic Algorithms," International Journal of Advanced Computer Science and Applications 2018;9(10).
[41] S. Petley and G. Aggidis, "Swansea bay tidal lagoon annual energy estimation," Ocean Engineering 2016;111;348-57.
[42] S. Bray, R. Ahmadian, and R. A. Falconer, "Impact of representation of hydraulic structures in modelling a severn barrage," Computers & Geosciences 2016;89;96-106.
[43] G.Aggidis and O.Feather, "Tidal range turbines and generation on the solway firth," Renewable Energy 2012;43;9-17.
[44] C. Baker, Tidal Power - Energy Engineering. Energy policy, 1991, p. 8.
[45] C. Baker and P. Leach, "Tidal lagoon power generation scheme in swansea bay," Report no. 14709570, 14709574. The Department of Trade and Industry and the Welsh Development Agency; 2006.
[46] R. Ahmadian and R. A. Falconer, "Assessment of array shape of tidal stream turbines on hydro-environmental impacts and power output," Renewable Energy 2012;44;318-27.
[47] J. Xia, R. A. Falconer, and B. Lin, "Impact of different tidal renewable energy projects on the hydrodynamic processes in the severn estuary, UK," Ocean Modelling 2010;32(1-2);86-104.
[48] B. Lin, J. M. Wicks, R. A. Falconer, and K. Adams, "Integrating 1D and 2D hydrodynamic models for flood simulation," Proceedings of the Institution of Civil Engineers - Water Management 2006;159(1);19-25.
[49] R. A. Falconer, "Flow and water-quality modelling in coastal and inland water," Journal of Hydraulic Research 1992;30(4);437-52.

[50] R. Ahmadian, R. A. Falconer, and B. Bockelmann-Evans, "Far-field modelling of the hydro-environmental impact of tidal stream turbines," Renewable Energy 2012;38(1);107-16.
[51] J. Xia, R. A. Falconer, B. Lin, and G. Tan, "Estimation of annual energy output from a tidal barrage using two different methods," Applied Energy 2012;93;327-36.
[52] J. Xia, R. A. Falconer, and B. Lin, "Impact of different operating modes for a severn barrage on the tidal power and flood inundation in the severn estuary, UK," Applied Energy 2010;87(7);2374-91.
[53] J. Xia, R. A. Falconer, and B. Lin, "Numerical model assessment of tidal stream energy resources in the severn estuary, UK," Proceedings of the Institution of Mechanical Engineers, Part A: Journal of Power and Energy 2010;224(7);969-83.
[54] "DiGSBS250K [SHAPE geospatial data], Scale 1:250000, Tiles: GB, Updated: 6 September 2011, BGS, Using: EDINA Geology Digimap Service, <http://digimap.edina.ac.uk>, Downloaded: 2017," ed.
[55] R. Ahmadian, C. Morris, and R. A. Falconer, "Hydro-environmental modelling of off-shore and coastally attached impoundments off the north wales coast," Proceedings of the 1st European IAHR Congress, United Kingdom;2010.
[56] J. Xia, R. A. Falconer, and B. Lin, "Hydrodynamic impact of a tidal barrage in the Severn Estuary, UK," Renewable Energy 2010;35(7);1455-1468.
[57] G. P. Evans, "A Framework for Marine and Estuarine Model Specification in the UK".1993.
[58] M. J. Lewis, A. Angeloudis, P. E. Robins, P. S. Evans, and S. P. Neill, "Influence of storm surge on tidal range energy," Energy 2017;122;25-36.
[59] A. Angeloudis, R. A. Falconer, S. Bray, and R. Ahmadian, "Representation and operation of tidal energy impoundments in a coastal hydrodynamic model," Renewable Energy 2016;99;1103-15.